Preparation and Characterization of Poly(*N*-*tert*-butylacrylamide-*co*-acrylamide) Ferrogel

Tuncer Caykara, Döne Yörük, Serkan Demirci

Department of Chemistry, Faculty of Art and Science, Gazi University, 06500 Besevler Ankara, Turkey

Received 21 January 2008; accepted 27 July 2008
DOI 10.1002/app.29095
Published online 23 January 2009 in Wiley InterScience (www.interscience.wiley.com).

ABSTRACT: Magnetic-field-sensitive gel, called ferrogel, was prepared by a two-step procedure in which first step requires synthesis of the poly(*N*-*tert*-butylacrylamide-*co*-acrylamide) [P(NTBA-*co*-AAm)] hydrogel and during second step magnetite (Fe_3O_4) particles were formed in the hydrogel via coprecipitation of Fe(II) and Fe(III) ions in alkaline medium at 70°C. The obtained ferrogel was characterized by attenuated total reflectance Fourier transform infrared spectroscopy, thermogravimetric analysis, scanning electron microscopy combined with energy dispersive spectroscopy, and electron spin resonance measurements. The magnetic responsive of the ferrogel was also investigated by applying magnetic field to the ferrogel. The extent of a bending degree of the ferrogel depends on the applied magnetic field strength. In addition, the magnetic responsive studies also indicated that formed magnetite content in the hydrogel is high enough to achieve considerable magnetic response to external magnetic field. As a result, the P(NTBA-*co*-AAm) ferrogel may be useful for potential applications in magnetically controlled drug release systems, magnetic-sensitive sensors, and pseudomuscular actuators. © 2009 Wiley Periodicals, Inc. J Appl Polym Sci 112: 800–804, 2009

Key words: poly(*N*-*tert*-butylacrylamide-*co*-acrylamide); magnetic field sensitive hydrogels; ferrogels

INTRODUCTION

Magnetic gels, called ferrogels, are a new class of stimuli-responsive polymeric materials with their properties controlled by magnetic field. These gels contain magnetic particles dispersed homogeneously or heterogeneously and confined in a polymer network. Under a nonuniform magnetic field, particles undergo motion, which in turn induces elongation, contraction, or bending of the gels with short response time.[1–7] The magneto-elastic properties of the ferrogels can be used to construct sensors, switches, and artificial muscles.[8–10] Their possible applications also include various separation and membrane and drug delivery system.[11–13]

There are two different methods to prepare ferrogel. One of them is the synthesis of magnetite (Fe_3O_4) and polymeric material separately followed by their combination through adsorption of polymeric chains onto a magnetite core or *vice versa*.[14–16] The other is the ion exchange between the counter ions in the electric double layer of the latex microbeads and metal ions followed by treatment with suitable chemicals for magnetic nanoparticle formation.[14,17]

In this work, a new two-step procedure was applied to prepare the ferrogel composed of crosslinked poly(*N*-tert-butylacrylamide-*co*-acrylamide) [P(NTBA-*co*-AAm)] and magnetite. First, the P(NTBA-*co*-AAm) hydrogel was synthesized by free-radical crosslinking copolymerization of corresponding monomers in methanol–water mixture. Subsequently, magnetic particles were formed in the hydrogel via coprecipitation of Fe(II) and Fe(III) in alkaline medium. The structure and properties of the obtained ferrogel were determined by attenuated total reflectance Fourier transform infrared (ATR-FTIR) spectroscopy, thermogravimetric analysis (TGA), scanning electron microscopy combined with energy dispersive spectroscopy (SEM/EDS), and electron spin resonance (ESR) spectroscopy. In addition, the bending behavior of the ferrogel under a magnetic field at various applied strengths was investigated for possible applications of magnetically controlled drug release systems and magnetochemical actuators and sensors.

EXPERIMENTAL

Materials

N-*tert*-Butylacrylamide (NTBA), acrylamide (AAm) *N*,*N*-methylenebisacrylamide (MBAAm), ammonium persulfate (APS), and *N*,*N*,*N*′,*N*′-tetramethylethylenediamine (TEMED) were purchased from Aldrich Chemical

Correspondence to: T. Caykara (caykara@gazi.edu.tr).

Company (Milwaukee, WI) Ferric chloride hexahydrate ($FeCl_3 \cdot 6H_2O$), ferric sulfate heptahydrate ($FeSO_4 \cdot 7H_2O$), potassium hydroxide (KOH), and potassium nitrate (KNO_3) were purchased from Merck (Darmstadt, Germany).

Preparation of P(NTBA-*co*-AAm) ferrogel

The P(NTBA-*co*-AAm) hydrogel was prepared by free-radical crosslinking copolymerization of NTBA and AAm in methanol–water mixture (1 : 1 v/v) at 20°C for 24 h. APS (0.056*M*) and TEMED (0.32*M*) were used as the redox initiator system. The NTBA (0.7 g), AAm (0.3 g), APS (2.0 mL), and 0.015 g MBAAm were dissolved in methanol (4.0 mL). The solution was purged with nitrogen gas for 10 min. After the addition of TEMED (2.0 mL), the solution was placed in poly(vinyl chloride) straw of 4 mm diameters and about 20 cm long. The poly(vinyl chloride) straw was sealed and immersed in a thermostated water bath at 20°C, and the copolymerization was conducted for 24 h. Upon completion of the reaction, the hydrogel was removed from the poly(vinyl chloride) straw and immersed in large excess of deionized water at room temperature for at least 72 h. The water was replaced 3–4 times every day to remove unreacted materials. After cleaning procedure, the swollen hydrogel was transferred into an aqueous solution containing $FeCl_3 \cdot 6H_2O$ (0.2*M*, 20 mL) and $FeSO_4 \cdot 7H_2O$ (0.1*M*, 20 mL) at room temperature for 10 days. After adsorption procedure, the metal ion-loaded hydrogel was treated with a mixture of KOH (0.5*M*, 50 mL) and KNO_3 (2.0*M*, 50 mL) at 70°C for 1 h, which resulted in the precipitation of the corresponding oxide, Fe_3O_4. The obtained ferrogel was finally washed with deionized water to neutral pH.

Characterization of ferrogel

ATR-FTIR measurements were made with a Nicolet 6700 FTIR (USA) spectrometer equipped with a smart orbit assessor in the range of 2000–500 cm^{-1}. Before the measurements, the originally swollen hydrogels were freeze-dried in a Virtis freeze drier (Lobconco, USA) for 2 days to completely remove water.

TGA was conducted with a TA instrument 2050 thermogravimetric analyzer. Freeze-dried samples were crashed into powder form by the aid of mortar and pestle and heated up to 800°C under N_2 atmosphere at a scan rate of 10°C/min.

SEM/EDS (JEOL, JSM-6360 LV, Tokyo, Japan) was used to study the internal or cross section morphology of ferrogel. Before the measurements, the swollen ferrogel at 22°C was firstly freeze-dried and then fractured and sputter coated with gold.

ESR spectra of the magnetite particles, the freeze-dried hydrogel and ferrogel were recorded by using a Varian E-line 9 spectrometer (Germany) with TE_{102} type double cavity resonator. ESR spectra of these samples were displayed in the form of the first derivative of the adsorption peak plotted against magnetic field. Spectrometer operating conditions are 9.3 GHz, 3.300 field set, 100 Hz field modulation, 1.0 G peak-to-peak modulation amplitude, and 1.0 mW microwave power to determine signal intensities, line widths, and *g*-values. All ESR signal intensities were performed by using DPPH standard sample.

The ferrogel prepared at cylindrical form was fixed vertically between the plane-parallel poles of an electromagnet (LakeShore Hall Effect System, EM4-HV Electromagnets and Model 450 Gaussmeter). The magnetic field was induced by steady current. The intensity of the current was varied between 0 and 10 A by an electronic device; the voltage was kept constant (40 V). The highest field strength used between the poles of the electromagnet was 1.3 Tesla. The magnetic response of the ferrogel was recorded by a video camera. The measurements were carried out at room temperature.

RESULTS AND DISCUSSION

The ferrogel composed of crosslinked P(NTBA-*co*-AAm) and Fe_3O_4 was prepared by using a two-step procedure. First, the hydrogel was synthesized by free-radical crosslinking copolymerization of NTBA and AAm in the presence of MBAAm as the crosslinker. Subsequently, magnetic particles were formed in the hydrogel via coprecipitation of Fe(II) and Fe(III) in alkaline medium. The chemical reaction of magnetite precipitation is expected as follows:

$$Fe^{2+} + 2Fe^{3+} + 8OH^- \xrightarrow{NO_3^-/\Delta} Fe_3O_4 + 4H_2O$$

The detailed investigations on the obtained ferrogel were performed by using ATR-FTIR spectroscopy, TGA, SEM/EDS spectroscopy, and ESR measurements. The ATR-FTIR spectra of the ferrogel, hydrogel, and Fe_3O_4 particles are illustrated in Figure 1. Both spectra were very similar and the following characteristic bands were identified: at $\sim$ 1227 and $\sim$ 1366 cm^{-1} [—$C(CH_3)_3$ groups of NTBA] and at 1665 cm^{-1} (amide I of both NTBA and AAm) and at 1610 cm^{-1} (amide II of both NTBA and AAm). There was only one new band at 850 cm^{-1}, specific for the stretching vibration of Fe—O groups from magnetite particles, which confirmed the hydrogel containing the magnetite seed particles, as also reported in the related literature.[18]

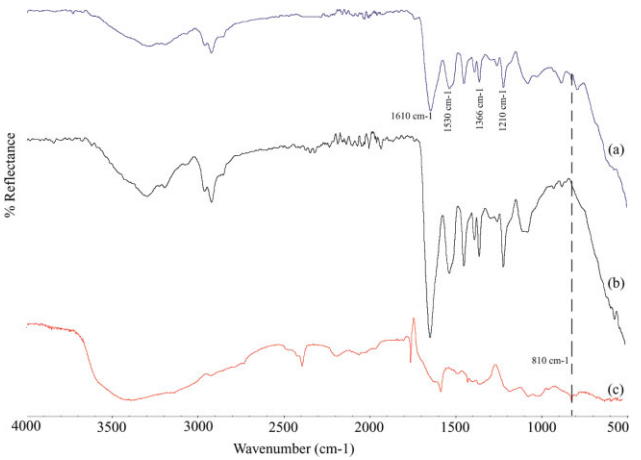

Figure 1 ATR-FTIR spectra of P(NTBA-*co*-AAm) + Fe_3O_4 (a), P(NTBA-*co*-AAm) (b), and Fe_3O_4 (c). [Color figure can be viewed in the online issue, which is available at www.interscience.wiley.com.]

Thermogravimetric analysis was employed to understand the thermal behavior and the metal loading capacity of the freeze-dried samples. Typical mass loss (TG) and derivative of mass loss (DTG) of the hydrogel and ferrogel are shown in Figures 2 and 3. From the TG curves, initial and final degradation temperatures were determined. From the DTG curves, the maximum temperature of mass loss was also noted. However, the mass loss of both the hydrogel and ferrogel started at ~ 344°C and reached to maximum at ~ 386°C. The TG curves of these samples indicated one reaction stage, which was reflected as single peak in the DTG curve. On the other hand, it can be said that the loading of metal particles for the hydrogel is quite high, ~ 10% by mass at 800°C, which was achieved on a single adsorption and reduction cycle bearing in mind that further loading of metal ions by multiple cycles of adsorption reduction procedures is also possible.

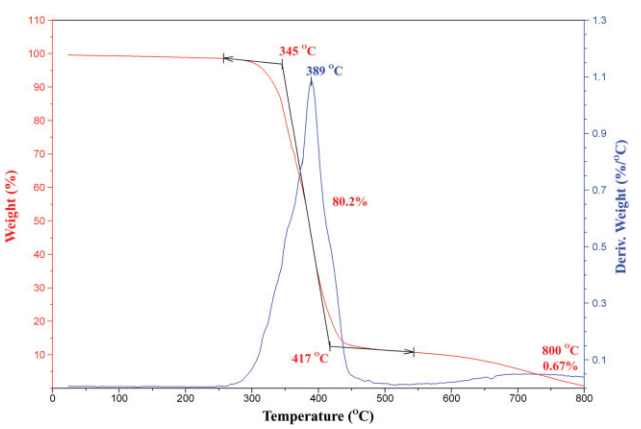

Figure 2 TGA and DTG thermograms of the hydrogel. [Color figure can be viewed in the online issue, which is available at www.interscience.wiley.com.]

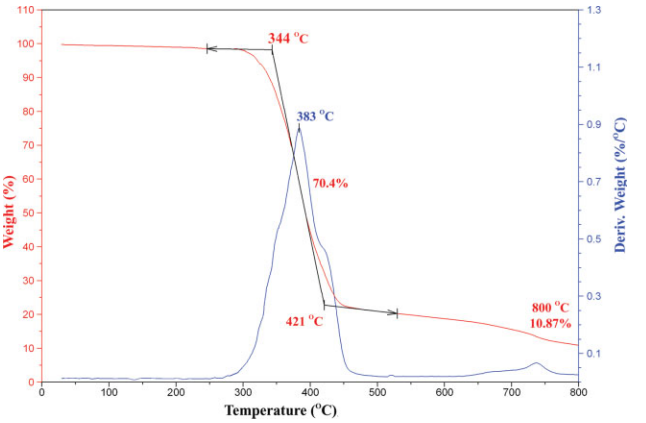

Figure 3 TGA and DTG thermograms of the ferrogel. [Color figure can be viewed in the online issue, which is available at www.interscience.wiley.com.]

SEM/EDS microanalysis was employed to determine the constitution of the magnetite particles dispersed in the hydrogel matrix. The surface (Fig. 4) and the cross-sectional (Fig. 5) micrographs of ferrogel (a), EDS Fe mapping (b), and EDS spectrum (c) are illustrated in Figures 4 and 5. The light spots on the EDS Fe mapping indicate the locations of Fe element. These spots were found to be randomly dispersed on both the ferrogel surface [Fig. 4(b)] and its inner part [Fig. 5(b)]. The EDS Fe mapping results are thus suggested to be dispersed heterogeneously in the ferrogel. Additionally, from the EDS spectra observations [Figs. 4(c) and 5(c)], it was noted that the Fe content on the surface of ferrogel is higher than that of its inner part.

The presence of magnetite particle in the ferrogel was also confirmed by ESR studies. Representative ESR spectra of the hydrogel, ferrogel, and magnetite particles are given in Figure 6. As shown in this

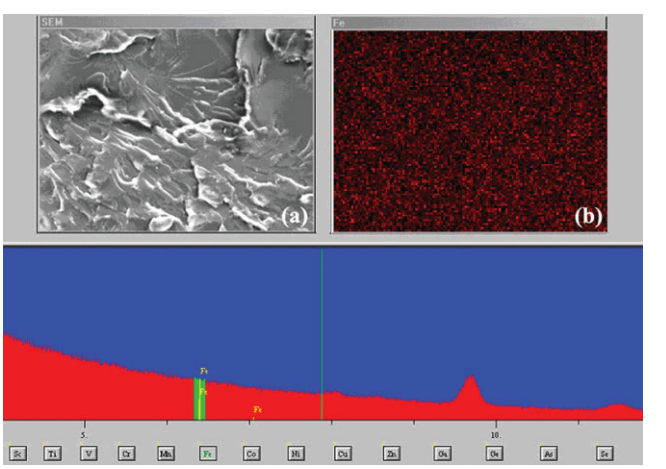

Figure 4 (a) The surface SEM micrograph (magnification: × 300), (b) EDS Fe mapping, and (c) EDS spectrum of the ferrogel. [Color figure can be viewed in the online issue, which is available at www.interscience.wiley.com.]

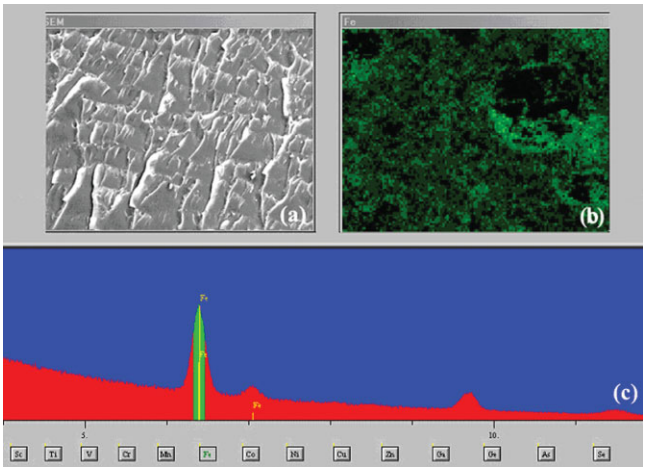

Figure 5 (a) The cross-sectional SEM micrograph (magnification × 300), (b) EDS Fe mapping, and (c) EDS spectrum of the ferrogel. [Color figure can be viewed in the online issue, which is available at www.interscience.wiley.com.]

figure, magnetite particles alone typically showed intensity of 24,100 around 2950 G applied magnetic field, whereas relative intensity of the ferrogel decreased to about 15,600 at the maximum which shifted to around 3330 G due to the effects of the hydrogel containing in the magnetite seed particles. Also note that the hydrogel did not exhibit any magnetic property as expected.

When a ferrogel is placed in a gradient of a magnetic field, torque and attractive force act on the magnetic particles, and the magnetic interactions are enhanced. The stronger field attracts the particles and due to their small size and strong interactions with molecules of dispersing liquid and polymer chains they all move together. Because of the cross-linking bridges in the network, changes in molecular conformation can accumulate and lead to macroscopic shape changes, which go together with motion. The principle of shape transformation and motility of ferrogel lies in an unique magnetoelastic behavior of such systems. The magnetic field drives and controls the motion, and this is in balance of magnetic and elastic interactions that determines the final shape. In this case, if a ferrogel cylinder is placed in a nonuniform magnetic field switching on and off periodically, where the average field gradient is perpendicular to the axis of the ferrogel, and the cylinder will bend periodically toward higher field strengths. This is demonstrated in Figure 7, which shows some photographs from the motion of the cylindrical ferrogel due to the magnetic field created by an electromagnet. The transition between straight and the curved forms—when turning off and on the magnetic field—is quick and reversible. The ferrogel can be made to bend and straighten repeatedly many times without damaging the gel. The ability of the ferrogel to undergo successive bending and stretching can be used to construct new types of soft actuators.

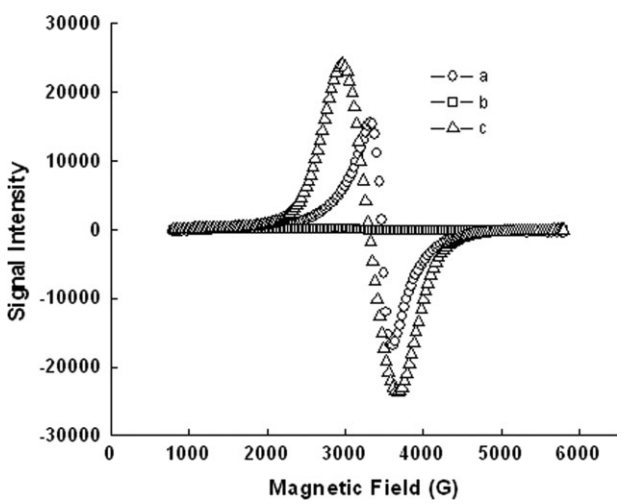

Figure 6 ESR spectra of the ferrogel (a), the hydrogel (b), and Fe_3O_4 particles (c).

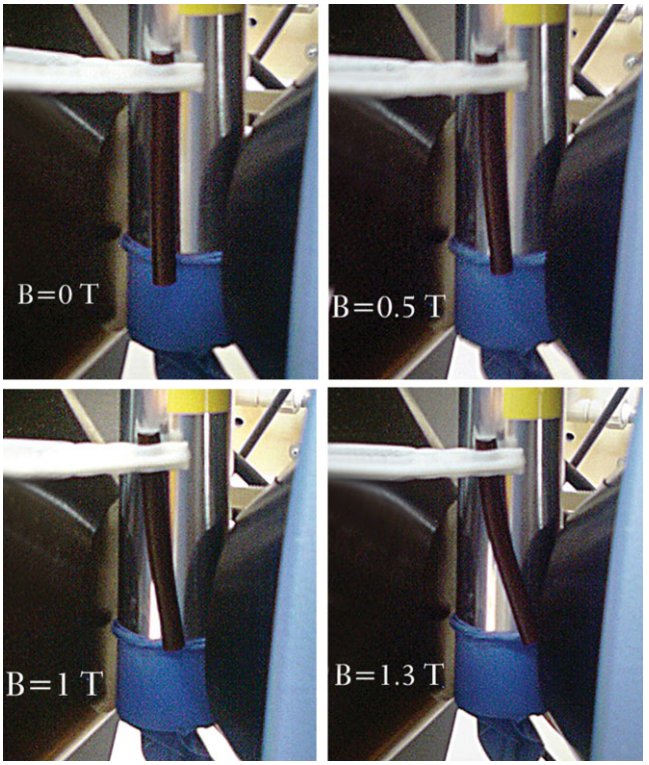

Figure 7 The photographs taken during the bending process under magnetic field of the ferrogel. The values of magnetic field are given in the photographs. [Color figure can be viewed in the online issue, which is available at www.interscience.wiley.com.]

CONCLUSIONS

In this study, a new route has been developed for the preparation of P(NTBA-*co*-AAm) ferrogel

containing Fe_3O_4. This route is based on a two-step procedure in which a hydrogel is prepared. Subsequent *in situ* synthesis of Fe_3O_4 in the hydrogel matrix then generates the magnetic field-sensitive ferrogel as evidenced from ATR-FTIR spectroscopy, TGA, and SEM/EDS spectroscopy. In addition, the magnetic behavior of ferrogel was also determined by applying of magnetic field and ESR measurements. It was observed that the bending degree of ferrogel depends on applied magnetic field strength. ESR curve measured for the ferrogel indicated that deposited magnetite content is enough to achieve considerable magnetic response to external magnetic field. As a result, this kind of ferrogel may have great potential in biomedicine such as catalysts, biosensors, hyperthermia applications, switchable electronic and signal-triggered delivery systems.

The authors thank Dr. Selim Acar for electromagnet measurements.

References

1. Torok, G.; Lebedev, V.; Cser, L.; Kali, G.; Zrinyi, M. Phys B 2001, 297, 40.
2. Szabo, D.; Czako-Nagy, I.; Zrinyi, M.; Vertes, A. J Colloid Interface Sci 2000, 221, 166.
3. Szabo, D.; Szeghy, G.; Zrinyi, M. Macromolecules 1998, 31, 6541.
4. Xulu, P.; Filipesei, G.; Zrinyi, M. Macromolecules 2000, 33, 1716.
5. Zrinyi, M.; Feher, J.; Filipesei, G. Macromolecules 2000, 33, 5751.
6. Zrinyi, M.; Barsi, L.; Buki, A. J Chem Phys 1996, 104, 8750.
7. Zrinyi, M.; Barsi, L.; Buki, A. Polym Gels Networks 1997, 5, 415.
8. Bckiari, V.; Pagosnis, K.; Bokias, G.; Lianos, P. Langmuir 2004, 20, 7972.
9. Lopes, D.; Cendoya, I.; Mijangos, C. Macromol Symp 2001, 166, 173.
10. Lao, L.; Ramanujan, V. R. J Mater Sci Mater Med 2004, 15, 1061.
11. Porter, J.; Pickup, R. W. J Microbiol Methods 1998, 33, 221.
12. Xie, X.; Zhang, X.; Zhang, H.; Chen, D.; Fei, W. J Magn Mater 2004, 277, 16.
13. Gupta, P. K.; Hung, C. T. Life Sci 1989, 44, 175.
14. Sahiner, N. Colloid Polym Sci 2006, 285, 283.
15. Sauzeddle, F.; Elaissari, A.; Pichot, C. Colloid Polym Sci 1999, 277, 846.
16. Gu, S.; Shiratori, T.; Konno, M. Colloid Polym Sci 2003, 281, 1076.
17. Zhang, J.; Coobs, N.; Kumacheva, E.; Lin, Y.; Sergant, E. H. Adv Mater 2002, 14, 1756.
18. Yamaura, M.; Camilo, R. L.; Sampaio, L. C.; Macedo, M. A.; Nakamura, M.; Toma, H. E. J Magn Mater 2004, 279, 210.